Electronic Supplementary Material (ESI) for Environmental Science: Nano.

Supporting Information for

Emerging investigator series: Aramid amphiphile nanoribbons for the remediation of lead from contaminated water

Ty Christoff-Tempesta, Julia H. Ortony*

Department of Materials Science and Engineering
Massachusetts Institute of Technology
Cambridge, MA, 02139, USA

* Correspondence to: ortony@mit.edu

Contents

1. Synthesis and chemical characterization

1a. Materials

Methyl 4-aminobenzoate (Sigma Aldrich, 98%), 3,3-dimethylbutyric acid (Sigma Aldrich, 98%), *N*-Boc-*p*-phenylenediamine (BPP, Sigma Aldrich, 97%), diethylenetriamine-*N,N,N″,N″*-tetra-*tert*-butyl acetate-*N′*-acetic acid (DTPA-tetra(t-Bu ester), Combi Blocks, 95%), 1-ethyl-3-(3-dimethylaminopropyl)carbodiimide hydrochloride (EDC, TCI Chemicals, 98%), 4-dimethylaminopyridine (DMAP, TCI Chemicals, 99%), 1-hydroxybenzotriazole hydrate (HOBt, TCI Chemicals, 97%), lithium hydroxide (LiOH, Alfa Aesar, 98%), sodium bicarbonate ($NaHCO_3$, Alfa Aesar, 99%), hydrochloric acid (HCl, Alfa Aesar, 36%), trifluoroacetic acid (TFA, Alfa Aesar, 99%), and 2-(4,7,10-tris(2-tert-butoxy-2-oxoethyl)-1,4,7,10-tetraazacyclododecan-1-yl)acetic acid (DOTA-tris(t-Bu ester), AstaTech, 95%), were used as received without further purification.

1b. Synthesis of compound 1

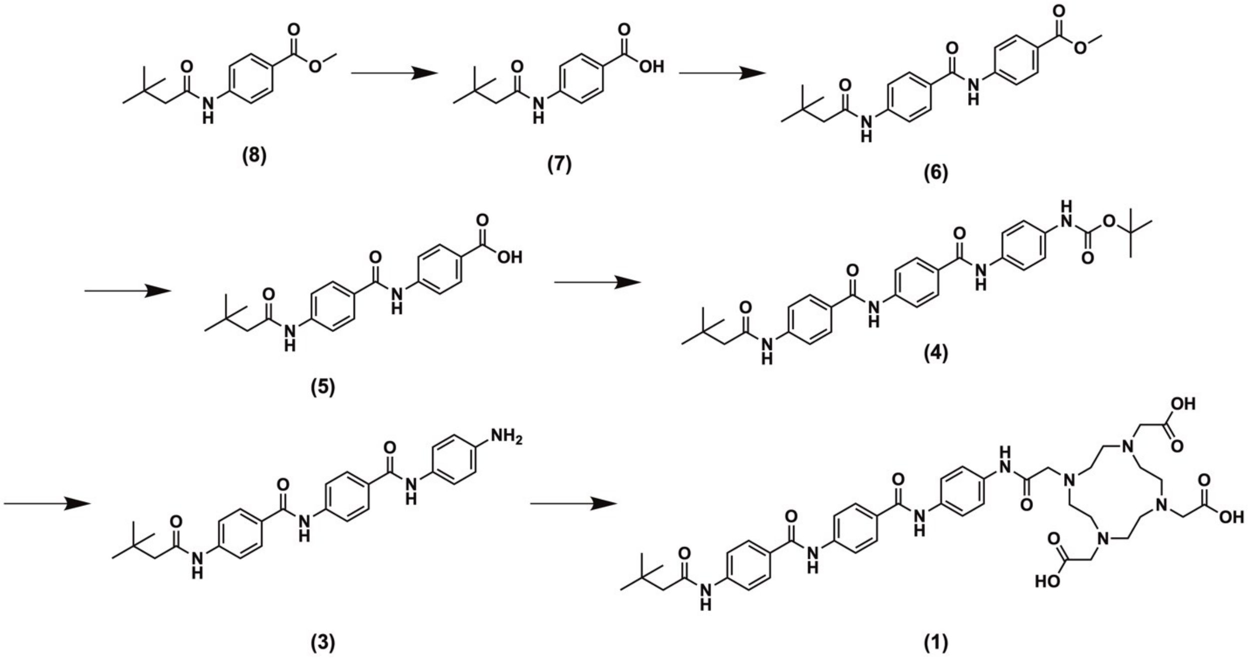

Scheme S1. Synthesis scheme to obtain the tetraxeten amphiphile.

Compound **3** was prepared as previously described.[25] For reference, we briefly outline the synthesis details to obtain this compound below:

Methyl 4-(3,3-dimethylbutanamido)benzoate (**8**): We mix a solution of methyl 4-aminobenzoate (11.01 mmol), 3,3-dimethylbutyric acid (16.52 mmol), EDC (33.03 mmol), and DMAP (33.03 mmol) in tetrahydrofuran (50 mL) for 24 h at room temperature. To obtain the final compound, the solvent was removed in vacuum, and the residue was washed with deionized water and extracted in chloroform. The final product was obtained by performing column chromotagraphy of the organic layer using silica gel and 1:1 ethyl acetate:hexane by volume (yield: 72%).

4-(3,3-dimethylbutanamido)benzoic acid (**7**): A mixture of 10 M LiOH (10 mL) and compound **8** (4.25 mmol) in ethanol (40 mL) was heated to 60°C and refluxed for 3 h, and then neutralized using an aqueous HCl solution. The precipitate was obtained by filtration and washed with water several times, and the resulting crude product was purified by reprecipitation from chloroform and methanol (yield: 98%).

Methyl 4-(4-(3,3-dimethylbutanamido)benzamido)benzoate (**6**): A mixture of EDC (6.37 mmol), DMAP (6.37 mmol), compound **7** (2.13 mmol), and methyl 4-aminobenzoate (6.37 mmol) in dimethylformamide (30 mL) was stirred for 24 h at 50 °C. To obtain the final product, the solvent was removed in vacuum and the remaining residue was precipitated in water. The crude mixture was collected by filtration, washed with excess methanol, and dried (yield: 83%).

4-(4-(3,3-dimethylbutanamido)benzamido)benzoic acid (**5**): A mixture of 10M LiOH (10 mL) and compound **6** (2.55 mmol) in tetrahydrofuran (20 mL) and ethanol (10 mL) was refluxed for 6 h and then neutralized with an aqueous HCl solution. To obtain the final product, the precipitate was filtered off, washed with water, and dried (yield: 98%).

tert-Butyl 4-(4-(4-(3,3-dimethylbutanamido)benzamido)benzamido)phenylcarbamate (**4**): A solution of compound **5** (0.85 mmol), BPP (2.55 mmol), EDC (2.55 mmol), and DMAP (2.55 mmol) in dimethylformamide (20 mL) was stirred at room temperature for 24 h. To obtain the final product, the solvent was evaporated, and then the crude mixture was washed with water and methanol (yield: 81%).

N-(4-(amino)phenyl)-4-(4-(3,3-dimethylbutanamido)benzamido)benzamide (**3**): A solution of TFA (500 µL) added dropwise into compound **4** (0.55 mmol) suspended in in methylene chloride (15 mL) was mixed for 6 h at room temperature. To obtain the final product, the volatile fraction was distilled off, the remaining mixture was washed with saturated $NaHCO_3$ solution, and the solid precipitate was filtered and dried (yield: 99%).

Full synthesis details to obtain compound **1** are provided here.

Synthesis of 2,2',2''-(10-(2-((4-(4-(4-(3,3-dimethylbutanamido)benzamido)benzamido)phenyl) amino)-2-oxoethyl)-1,4,7,10-tetraazacyclododecane-1,4,7-triyl)triacetic acid (**1**): A solution of **3** (1.35 mmol), DOTA-tris(t-Bu ester) (1.62 mmol), EDC (4.05 mmol), and DMAP (4.05 mmol) in dimethylformamide (20 mL) was stirred at 60 °C for 24 h. After the reaction, the solvent was removed *in vacuo*. The residue was suspended in deionized water and filtered to obtain a light-yellow precipitate. The isolated compound was then reacted with TFA (8 mL) in chloroform (20 mL) for 17 h. The volatile fraction was evaporated under reduced pressure. The remaining residue was suspended in ethyl acetate and filtered to obtain compound **1** by filtration (yield: 43%). ^1H NMR (400 MHz, Bruker Avance III DPX 400, DMSO-*d*): 7.95 (m, 8H), 7.75 (t, 4H), 7.57 (d, 2H), 4.04 (m, 1H), 3.88 (s, 6H), 3.74 (s, 3H), 3.63 (s, 1H), 2.7 (m, 4H) , 2.25 (s, 2H), 2.00 (s, 1H), 1.91

(s, 1H), 1.17 (m, 2H), 1.05 (s, 9H) ppm. MS (MALDI-ToF) $[M + H]^+$ m/z calculated: 831.40; $[M + H]^+$ found: 831.41.

Mass spectrometry experimental details: The molecular weight of **1** was determined using a Bruker Omniflex matrix assisted laser desorption/ionization-time-of-flight (MALDI-ToF) instrument with a Reflectron accessory. The matrix solution used α-cyano-4-hydroxycinnamic acid in 50:50:0.1 water:acetonitrile:TFA by volume. SpheriCal Peptide Low (Polymer Factory) was added to the MALDI-ToF solution as an internal calibrant.

1c. Synthesis of compound 2

Compound **2** was prepared as previously described.[25] For reference, we briefly outline the synthesis details to obtain this compound below:

2,2',2'',2'''-((((2-((4-(4-(4-(3,3-dimethylbutanamido)benzamido)benzamido)phenyl)amino)-2-oxoethyl)azanediyl)bis(ethane-2,1-diyl))bis(azanetriyl))tetraacetate (**2**): A solution of compound **3** (0.29 mmol), EDC (1.17 mmol), DMAP (1.17 mmol), and DTPA-tetra(t-Bu ester) (0.58 mmol) in dimethylformamide (20 mL) was stirred at 50 °C for 72 h. After the reaction, the solvent was removed in vacuum and the remaining residue was purified by flash column chromatography using silica gel and 7:1 tetrahydrofuran:chloroform (by volume). The resulting compound was mixed with TFA (500 μL) and methylene chloride (15 mL) for 48 h. To obtain the final product, the volatile fraction was removed by vacuum, and tetrahydrofuran was added to suspend the product, which was collected by filtration and dried (yield: 67%).

2. Experimental details

Sample preparation: Nanoribbon suspensions were prepared by dissolving compounds **1** and **2** in deionized water and sonicating for ten minutes in a bath sonicator. Lead solutions were prepared by dissolving lead (II) nitrate (99.999% trace metals basis, Sigma-Aldrich) in deionized water. The concentrations of lead stock solutions were verified by ICP-MS.

Transmission Electron Microscopy (TEM): Self-assembled nanostructures were observed by TEM using a FEI Tecnai G2 Spirit TWIN microscope at a 120 kV accelerating voltage. TEM grids were prepared by depositing 7.0 µL of a 1 mg/mL amphiphile solution onto a continuous carbon grid (Electron Microscopy Sciences, 200 mesh, copper) for 30 sec, blotting to remove the solution, depositing 7.0 µL of a 1% phosphotungstic acid aqueous solution (Electron Microscopy Sciences) onto the grid, and blotting to remove the stain.

Cryogenic Transmission Electron Microscopy (Cryo-TEM): Cryo-TEM images were captured on a Talos Arctica G2 Cryo-TEM at a 200 kV accelerating voltage. Grids were prepared with an FEI Vitrobot Mark IV. To prepare a sample for analysis, 3.0 µL of a 1.0 mg/mL nanoribbon solution was pipetted onto a glow-discharged holey carbon grid (Ted Pella, 300 mesh, copper) in a chamber set to 100% humidity. The grids were blotted for 4 sec and then immediately plunged into liquid ethane and subsequently retained in liquid nitrogen.

Small Angle X-Ray Scattering (SAXS): SAXS profiles of aqueous nanoribbon solutions were captured at Beamline 12-ID-B of the Advanced Photon Source at Argonne National Laboratory using a 13.3 keV X-Ray radiation energy and DECTRIS PILATUS 300K detector. Solutions were loaded into 2 mm diameter quartz capillary tubes (Hampton Research) for analysis. Reported SAXS profiles were background subtracted using beamline software to subtract water and capillary background.

Ultraviolet-Visible (UV-Vis) Spectroscopy: UV-Vis absorbance profiles of aqueous amphiphile solutions with variable Pb^{2+} concentrations were captured on a PerkinElmer LAMBDA 850+ UV/Vis spectrophotometer. The amphiphile concentration was fixed at 0.05 mM.

Isothermal Titration Calorimetry (ITC): Binding isotherms were captured on a Microcal VP-ITC ultrasensitive titration calorimeter. A 3.0 mM lead nitrate aqueous solution was injected into 0.3 mM nanoribbon solutions prepared from the same deionized water source. A buffer was not used due to the insolubility of lead species in most buffers. The ITC was run with 5 µL injection intervals over 10 seconds in five minute intervals at 25 ºC. Titrations were carried out three times to ensure consistency and reproducibility. Data analysis was conducted using instrument software.

Adsorption Isotherms: Lead concentrations used to construct adsorption isotherms were analyzed on an Agilent 7900 inductively coupled plasma-mass spectrometer (ICP-MS). Concentration calibration curves were constructed using a 1 ppm lead ICP-MS stock solution from Ricca Chemical. Internal calibration for each sample used a 10 ppm rhodium ICP-MS stock solution from Sigma-Aldrich. Calcium chloride, copper chloride, magnesium sulfate, and nickel chloride salts were obtained from Sigma-Aldrich. Adsorption isotherm solutions were mixed for 24 h before analysis. After 24 h, the solutions were centrifuged for 5 min. at 10,000 rcf and the supernatant was retained for testing.

3. Small-angle X-ray scattering of compound (1) nanostructures

A SAXS profile of an aqueous suspension of compound **1** is shown in Fig. S1. The best fit to this data, a lamellar_headgroup bilayer model, is shown in red; other fits attempted included a rectangular prism, a rectangular prism_headgroup, cylindrical, and cylindrical_headgroup models. Models with the "_headgroup" suffix allow for discrete scattering length densities (SLDs) for the core and head group domains of the structure. The model shown in Fig. S1 uses a solvent (water) SLD of 9.44 x 10^{-6} Å^{-2}, head group SLD of 8.13 x 10^{-6} Å^{-2}, and core SLD of 12.53 x 10^{-6} Å^{-2}, based on calculations from the chemical formulas and structures of these regions. The lamellar fit returns a combined head group length of 1.1 nm and a core thickness of 2.8 nm, for a total 3.9 nm thickness. This model is unable to resolve a nanoribbon width dimension, so we rely on Cryo-TEM to determine width. SAXS fitting of compound **2** is reported elsewhere.[25]

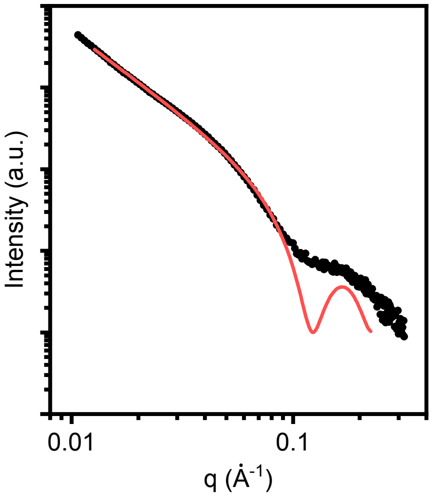

Fig. S1. SAXS of an aqueous suspension of compound **1** nanoribbons is fit to a lamellar model (red), which returns a 3.9 nm nanoribbon thickness.

4. Maintenance of nanoribbon morphology with lead chelation

Nanoribbons produced from the self-assembly of compounds **1** and **2** maintain their nanostructure upon the chelation of lead, as shown in Fig. S2. Compound **1** nanoribbons are observed in an aggregated state.

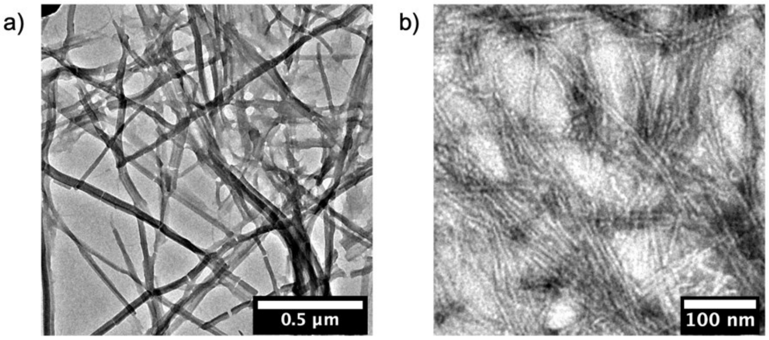

Fig. S2. (a) Compound **1** and (b) compound **2** nanoribbons after the chelation of lead.

5. Stability of nanoribbons against changes in pH

Environmental pH can be used to modify the morphology of amphiphilic self-assembling systems by changing the charge and effective head group size of the amphiphiles. However, we hypothesized the AA system may be stable against perturbations to environment post-assembly due to the stability imparted to the nanostructures by the aramid structural domain. TEM of nanoribbons introduced to a pH 3 environment show no change in morphology after 24 h at this pH (Fig. S3). These nanoribbon suspensions were not sonicated after pH adjustment, so the nanoribbons may retain a morphology away from their equilibrium state.

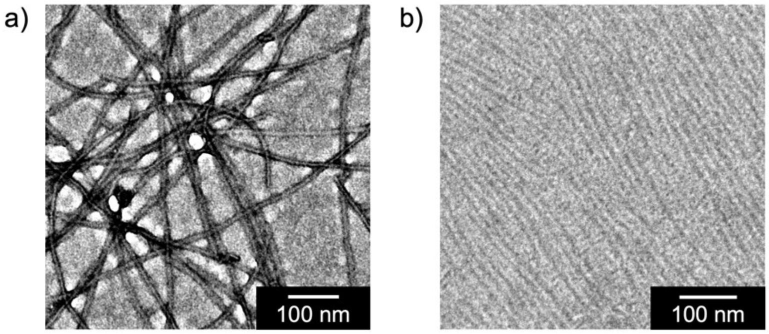

Fig. S3. (a) Compound **1** and (b) compound **2** nanoribbons retain their morphology after adjustment of the aqueous environment to pH 3.

6. Fits of adsorption isotherm curves to a Langmuir model

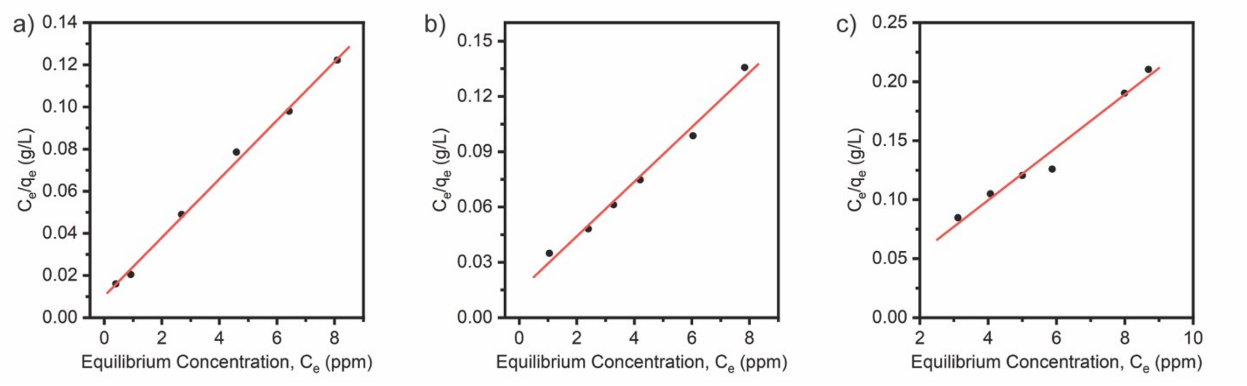

Fig. S4. Linear regression of pH-dependent lead adsorption for compound **1** obtained by fitting equilibrium data to a Langmuir adsorption model, accompanying Fig. 3c of the main text. The fittings shown here are for (a) pH 7, (b) pH 5, and (c) pH 3.

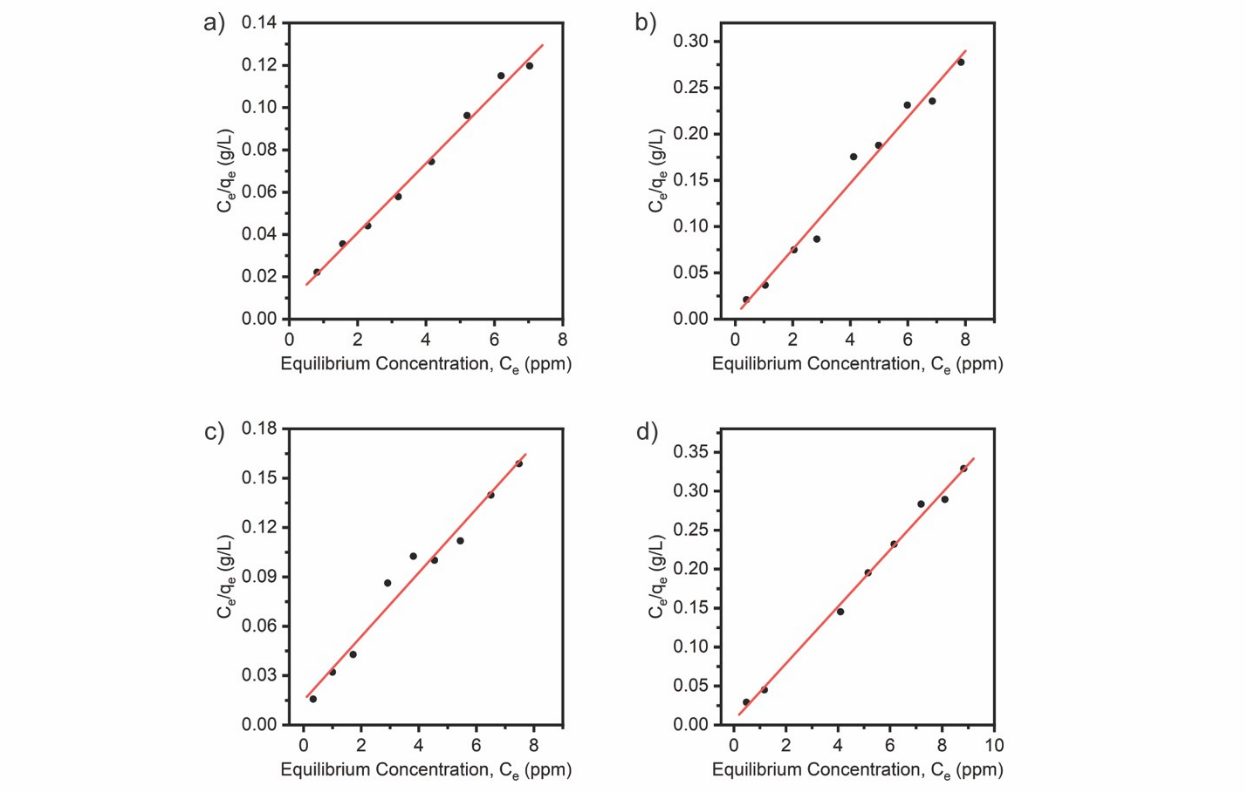

Fig. S5. Linear regression of competing counterion lead adsorption for compound **1** obtained by fitting equilibrium data to a Langmuir adsorption model, accompanying Fig. 3d of the main text. The fittings shown here are for Pb^{2+} adsorption when present in equimolar quantities with (a) Ca^{2+}, (b) Cu^{2+}, (c) Mg^{2+}, and (d) Ni^{2+}.

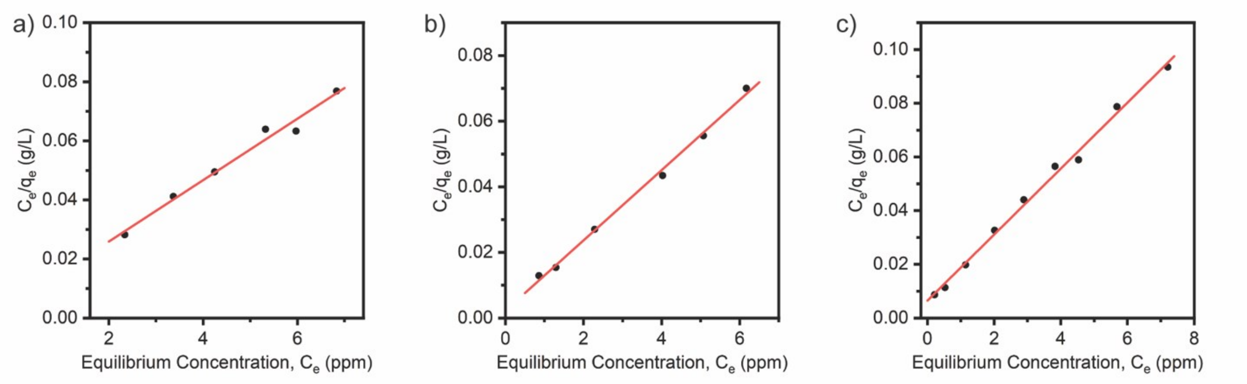

Fig. S6. Linear regression of pH-dependent lead adsorption for compound **2** obtained by fitting equilibrium data to a Langmuir adsorption model, accompanying Fig. 4c of the main text. The fittings shown here are for (a) pH 7, (b) pH 5, and (c) pH 3.

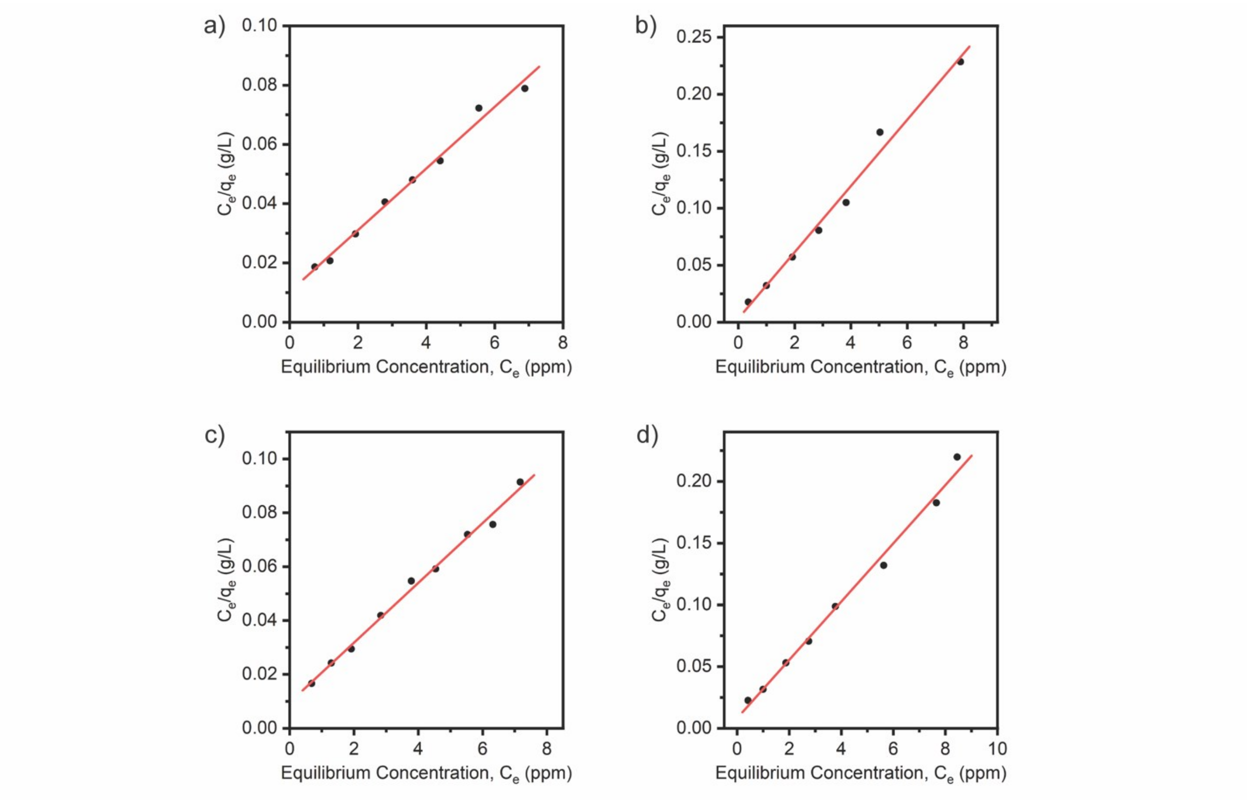

Fig. S7. Linear regression of competing counterion lead adsorption for compound **2** obtained by fitting equilibrium data to a Langmuir adsorption model, accompanying Fig. 4d of the main text. The fittings shown here are for Pb^{2+} adsorption when present in equimolar quantities with (a) Ca^{2+}, (b) Cu^{2+}, (c) Mg^{2+}, and (d) Ni^{2+}.